余星,许绪成,李洪林等. 2023. 红海及周边地质构造特征与地球动力学演化. 岩石学报,39(03): 731 - 741, doi: 10.18654/1000 - 0569/2023.03.07

红海及周边地质构造特征与地球动力学演化*

余星[1,2] 许绪成[1] 李洪林[1] 韩喜球[1,2,3] 胡航[1] 何虎[1] 余娅娜[1]

YU Xing[1,2], XU XuCheng[1], LI HongLin[1], HAN XiQiu[1,2,3], HU Hang[1], HE Hu[1] and YU YaNa[1]

1. 自然资源部海底科学重点实验室,自然资源部第二海洋研究所,杭州 310012
2. 浙江大学海洋学院,舟山 316021
3. 上海交通大学海洋学院,上海 200240

1. *Key Laboratory of Submarine Geosciences*, *Second Institute of Oceanography*, *Ministry of Natural Resources*, *Hangzhou* 310012, *China*
2. *Ocean College*, *Zhejiang University*, *Zhoushan* 316021, *China*
3. *School of Oceanography*, *Shanghai Jiao Tong University*, *Shanghai* 200240, *China*

2022-06-01 收稿, 2022-11-16 改回.

Yu X, Xu XC, Li HL, Han XQ, Hu H, He H and Yu YN. 2023. The geotectonic characteristics and geodynamic evolution of the Red Sea Rift and its adjacent areas. *Acta Petrologica Sinica*, 39(3): 731 - 741, doi: 10.18654/1000-0569/2023.03.07

Abstract The Red Sea is the youngest ocean on Earth, and it is currently in the juvenile ocean basin stage of the Wilson cycle. Its two ends are connected to the East African Rift in the south and the Mediterranean in the north, representing the embryonic and terminal stages, respectively. Due to its unique geographical and tectonic location, the Red Sea is an ideal location for the study of plate tectonics. Through comprehensive analysis of available geological, geophysical and geochemical data, we can reexamine the topography, gravity and magnetic anomalies, as well as the along-axis geochemistry of the basalts. This can help to determine the distribution of oceanic crust, the evolution history of the Red Sea Rift, and the heterogeneity of the mantle source. The Red Sea is deeper in the middle and shallower in the two ends, and it can be divided into four sections: the north, the central-north, the central-south and the south. The stripes of the gravity and magnetic anomalies are mainly observed in the central-south section instead of the other sections, which astricts the previous understanding of the Red Sea's spreading history. It is currently believed that there is an oceanic crust throughout the entire Red Sea. The coastal escarpments on both sides of the Red Sea represent conjugate rifted continental margins that form a horn-shaped opening to the south, as opposed to the spindle-shaped spreading outlined by the coastline. The along-axis geochemical compositions of the basalts from the Red Sea Rift indicate the mantle source heterogeneity. Enriched MORBs were sampled from the southern section, suggesting the influence of the Afar plume. The Red Sea Rift has undergone three major stages of evolution: pre-rift volcanism (31 ~ 29Ma), continental rifting (29 ~ 13Ma), and oceanic spreading (< 13Ma). The formation and evolution of the Red Sea Rift are closely related to the breakup of Arabian plate from the African continent, the activity of Afar plume and the closure of New Tethys Ocean. The study of the geodynamic process of the Red Sea Rift provides a basis for understanding the geotectonic evolution and plate movement of the region.

Key words Red Sea Rift; Geotectonic characteristics; Evolution history; Mid-ocean ridge basalt; Geochemistry; Geodynamics

摘 要 红海是地球上最年轻的大洋,其板块构造活动正处于威尔逊旋回的幼年期。红海南北两端分别连接着威尔逊旋回的胚胎期和终结期,即东非大裂谷和地中海。这一独特的地理位置和构造部位使其成为板块构造理论研究的圣地。本文通过对已有的地质、地球物理和地球化学资料进行综合分析,了解了红海地区的地形、重磁异常和沿脊的玄武岩地球化学组成等地质构造特征,探讨了红海裂谷的洋壳分布、地幔源区不均一性以及扩张演化历史等问题。红海地形中间深、南北两端浅,可以分为北、中北、中南、南等四段。重磁异常的条带主要出现在中南段,其他段不明显,因而限制了以往对红海扩张历史

* 本文受国家重点研发计划课题(2021YFF0501301),国家自然科学基金项目(42172231、41872242)和自然资源部第二海洋研究所基本科研业务费专项(QNRC2202)联合资助.

第一作者简介: 余星,男,1981 年生,研究员,博士生导师,从事岩石大地构造学研究. E-mail: yuxing@sio.org.cn

的认识。目前认为红海全段存在洋壳,红海两岸的沿岸悬崖是共轭扩张陆缘,呈向南开口的喇叭型扩张,而非对应红海岸线的梭子型。红海裂谷沿脊的地幔源区具有明显的不均一性,南段玄武岩显示 E-MORB 特征,表现为阿法尔地幔柱的影响。红海的发育经历了裂谷前火山作用(31~29Ma)、大陆张裂(29~13Ma)和洋底扩张(<13Ma)三个主要阶段。红海裂谷的形成演化与非洲大陆的裂解、阿法尔地幔柱的活动、新特提斯洋的闭合等密切相关,了解红海的地球动力学过程将为揭示区域大地构造演化以及板块运动规律提供依据。

关键词 红海裂谷;地质构造特征;演化历史;洋中脊玄武岩;地球化学;地球动力学

中图法分类号 P541; P542

红海是位于非洲与阿拉伯半岛之间的一个 NNW-SSE 走向的狭长海域,因季节性繁殖红藻而得名(Belogorskaya, 1970)。围绕红海的调查和研究工作始于 1869 年苏伊士运河的开通,1881 年苏联 Vityaz 号科考船首次测量了红海海水和沉积物的盐度和温度,1897 年奥地利 Pola 号科考船首次采集到了红海海底红褐色的多金属软泥。1950-1960 年,美苏英德法等国在红海开展了大量的地质和地球物理调查,1984 年德国 Sonne 号科考船首次在红海采集到了块状硫化物样品(Scholten *et al.*,2000)。截至目前,人们对红海海底的地形地貌、构造演化、深部结构、海底沉积、成矿作用和生物资源等众多问题,都有了较深入的认识(Girdler, 1958; Mckenzie *et al.*, 1970; Le Pichon and Francheteau, 1978; Bonatti *et al.*, 1984; Roger, 1993; Bosworth *et al.*, 2005; Augustin *et al.*, 2014, 2019, 2021; Almalki *et al.*, 2015, 2016; Bosworth, 2015)。不过,目前有关红海裂谷的洋壳分布范围、扩张历史、裂谷分段、地幔源区不均一性、洋脊-地幔柱相互作用等问题仍存在较大争议。

红海裂谷代表了威尔逊旋回的幼年期,指示新生大洋的开始,南部与胚胎期的东非大裂谷及幼年期的亚丁湾紧密相连,北部与终年期的地中海相接,具有独特的构造位置。红海连接着印度洋、地中海与大西洋,是沟通亚非欧三洲的战略要道。但我国对红海地区的研究比较滞后,尚未开展过直接的海洋地质调查,已有研究主要基于国外已有的调查资料(黄彦庆和侯读杰,2006; 曾志刚,2011; 李家彪,2017; 李三忠等,2018),对红海的关注和研究程度明显不足。本文基于已有的调查研究资料,进一步梳理红海的地质构造特征,包括地形地貌、重磁异常、地壳属性、岩石地球化学特征等,重点探讨红海裂谷的分段、洋壳分布、扩张历史和地幔源区不均一性等问题。研究将为认识红海周边陆块的活动、冈瓦纳大陆的裂解、陆洋转换过程以及新生大洋的构造岩浆活动等提供支撑,为理解板块构造运动规律提供帮助。

1 红海地形地貌特征及裂谷分段

红海处于非洲板块与欧亚板块的交接部位,北端以西奈半岛为界,经苏伊士运河与地中海相连,南端经曼德(Bab-el-Mandeb)海峡与亚丁湾相接,南北两端窄、中间宽,呈梭子型(图 1)。红海的纬度范围约 12.5°~28°N,全长约 2000km,最宽处 355km,面积约 44 万 km^2(Head, 1987; Rasul *et al.*, 2015)。红海平均水深 490m,从近岸到轴部水深变深,呈现中央裂谷特征。轴部裂谷狭窄,大于 1000m 水深区域的平均宽度约 50km。裂谷中心发育间隔排列的海渊,集中分布于 19°~23°N 裂谷段(Bäcker and Schoell, 1972; Scholten *et al.*, 2000; Augustin *et al.*, 2014; Brueckmann *et al.*, 2017)。位于 19°40′N 的萨瓦金(Suakin)海渊为红海最深点,水深 2860m(图 1、图 2)。从萨瓦金海渊向南北两侧延伸,水深变浅,并且南侧变化幅度更大,到曼德海峡最大水深不足 250m(图 2)。

红海裂谷未见有明显的转换断层边界,因此其分段存在诸多不确定性。目前主要依据地形地貌及重磁等资料进行划分。Cochran *et al.*(1986)将红海分为北段、中段和南段三部分,分界线分别在 25°N 和 20°N,南段至 15°N 止。Almalki *et al.*(2015)将 Onib-Hamisana 缝合带视为北段与中段的边界,Baraka 缝合带作为中段与南段的边界,并在 15°N 以南识别出洋脊跃迁作用,将跃迁后的洋脊段称为阿法尔段。15°N 以南区域裂谷发育不明显,且缺少磁条带,因此在前人的划分中常常被忽略。

本研究基于前人的分段结果,并综合地形、重磁以及地球化学资料,将红海整体分为四段,分别为北段、中北段、中南段和南段(图 2)。北段从西奈半岛默罕默德角至 Onib-Hamisana 缝合带,全长约 500km;中北段从 Onib-Hamisana 缝合带至 Baraka 缝合带,全长约 460km;中南段从 Baraka 缝合带至 17°N 附近的 Farisan-Dahlak 断裂带,全长约 440km。这三段与前人的划分基本一致。从 17°N 至曼德海峡视为红海南段,全长约 600km。南段具有明显不同于其他段的地球化学特征,且洋脊在此处发生跃迁,跳过达纳基尔(Danakil)地块西移至 Manda Hararo 裂谷(Almalki *et al.*,2015)。

2 红海重磁异常特征及洋壳分布

红海的重磁异常观测始于十九世纪末,在二十世纪五、六十年代进入调查高峰期。1958 年,美国 Vema 号科考船对红海进行了第一次磁异常测量。1963 年编制了整个红海区域的布格重力异常图(Phillips *et al.*, 1969)。Allan(1970)、Hall(1979)和 Cochran(1983)等先后对红海的磁异常进行了调查研究,并绘制了红海的洋壳磁异常等时线。Makris *et al.*(1991)、Cochran(2005)和 Almalki *et al.*(2016)等利用重力异常数据分析了红海的地壳结构。Ligi *et al.*(2012)通过磁

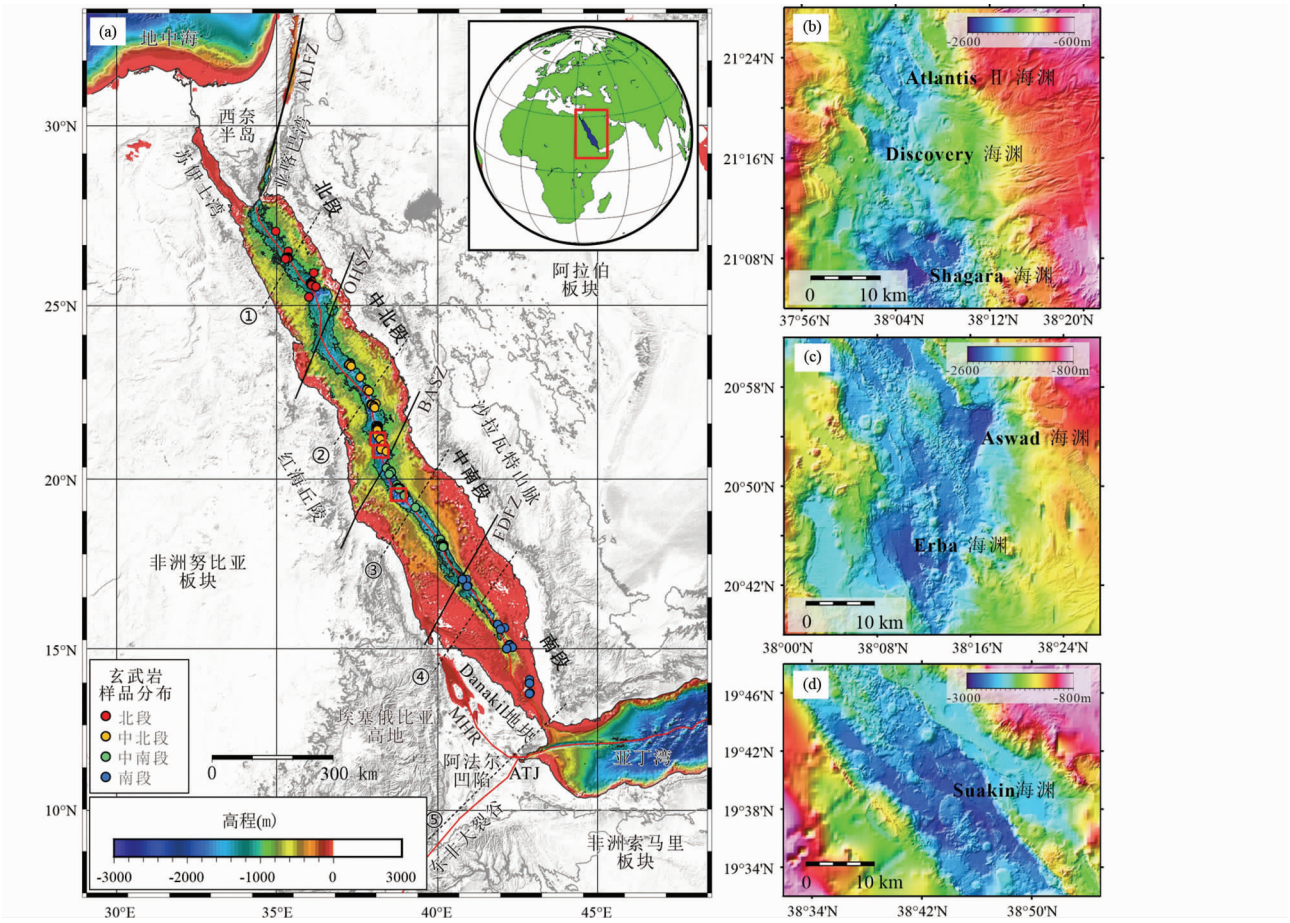

图 1　红海裂谷及周边地形地貌图

(a)红海水深图,右上角插图指示红海位置;水深数据来自 GEBCO,分辨率 30 弧秒,陆地地形数据来自 SRTM15 + 网格数据,分辨率 15 弧秒(Tozer *et al.*,2019). 显示的陆地等高线为 1000m,红海等深线为 – 1000m,沿中央裂谷的红线为扩张中心,横贯裂谷的黑色虚线指示图 2 的横剖面位置(带编号). 黑色实线为分段边界:ALFZ-亚喀巴-黎凡特(Aqaba-Levant)断层,OHSZ-Onib-Hamisana 缝合带,BASZ-Baraka 缝合带,FDFZ-Farasan-Dahlak 断裂带;ATJ-阿法尔三联点,MHR-Manda Hararo 裂谷带. (b-d)中央裂谷上的典型海渊地形特征,位置见图 1a 中的 3 个小红框

Fig. 1　Topographic map of the Red Sea Rift and its adjacent areas

(a) bathymetric map of the Red Sea with an inset indicating its location. The bathymetric data are from GEBCO with a resolution of 30 arc seconds, while the terrestrial topographic data are from SRTM15 + with a resolution of 15 arc seconds (Tozer *et al.*, 2019). The shown contours on land are at 1000m, in the Red Sea at – 1000m. The red line along the rift axis indicates the spreading center. The numbered black dashed lines across the rift indicate the location of profiles in Fig. 2. The solid black lines are the segment boundaries: ALFZ-Aqaba-Levant Fracture Zone, OHSZ-Onib-Hamisana Suture Zone, BASZ-Baraka Suture Zone, FDFZ-Farasan-Dahlak Fracture Zone; ATJ-Afar Triple Junction, MHR-Manda Hararo Rift Zone. (b-d) typical topographic features of the deeps in the rift valley. The locations of the maps are shown as three small red boxes in Fig. 1a

异常观察认为红海中的洋壳侵位由南向北传播。Saada *et al.*(2021)综合重磁和地形数据,认为红海南段已完全进入海底扩张阶段,而北段处于扩张初期,仍存在陆壳,中段为过渡段。Issachar *et al.*(2022)利用船磁和卫星磁力数据,编制了新的红海磁力异常图,发现整个红海存在沿轴的磁异常区,并且发育近垂直于脊轴的异常带。

由于红海规模较小,尚处于大洋形成的幼年期,磁条带分布十分局限,加之裂谷内沉积层较厚,引起地球物理探测资料的多解性,目前关于红海中洋壳的分布范围仍存在很大争议。中南段明显的重磁异常条带可以证实洋壳的存在(Hall,1979;Cochran,1983; Izzeldin,1987),但中南段洋壳分布的宽度以及 20°N 以北区域是否存在洋壳仍不明确。大部分观点认为 20°N 以北区域为陆壳或过渡地壳(Bosworth *et al.*,2005; Almalki *et al.*,2015; Schettino *et al.*,2016; Saada *et al.*,2021)。也有观点认为北部区域存在零星的洋壳,在海渊中出露,而海渊之间由陆壳间隔(Coleman and McGuire, 1988;Cochran,2005)。

综合前人的重磁调查研究资料,结合 Sandwell *et al.*(2014)的全球海洋重力模型和全球地磁异常网格数据 EMAG2(Meyer *et al.*,2017),可以发现,红海的中南段具有明

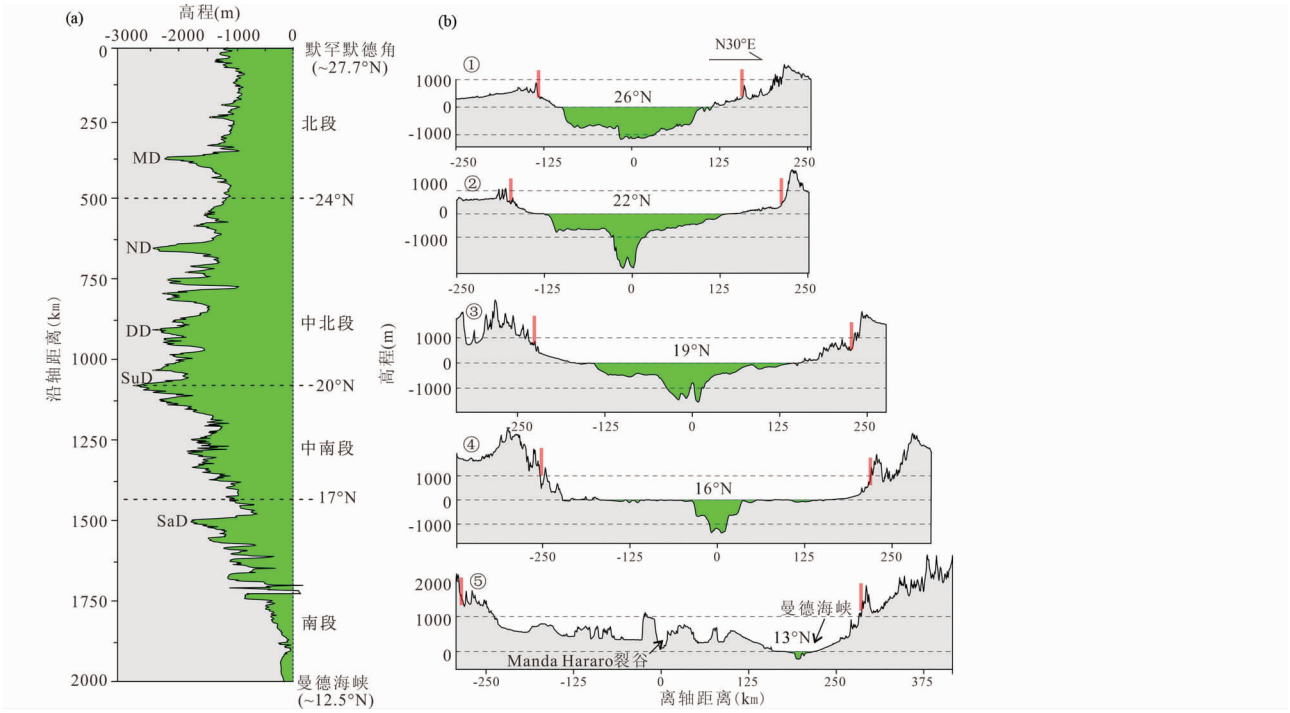

图 2 红海裂谷轴向及横向地形剖面图

(a)沿轴水深变化图,粗虚线代表分段界线. MD-Mabahiss 海渊,ND-Nereus 海渊,DD-Discovery 海渊,SuD-Suakin 海渊,SaD-Saso 海渊. (b)红海裂谷不同部位的横向地形剖面,剖面方向近似裂谷扩张方向,红色粗线段指示推测的共轭陆缘(沿岸悬崖);剖面上的纬度值代表剖面与裂谷中心的交叉点纬度,具体剖面位置见图 1a

Fig. 2 Bathymetric variation along the axis and across specific profiles of the Red Sea Rift

(a) bathymetric variation along the axis. The thick dashed line represents the segment boundaries. MD-Mabahiss deep, ND-Nereus deep, DD-Discovery deep, SuD-Suakin deep, SaD-Saso deep. (b) lateral topographic profiles across different rift segments of the Red Sea. The red bars indicate the speculated conjugate land margins (coastal escarpment). The labeled latitude represents the intersection of the profile with the rift axis. The specific locations of all the profiles are shown in Fig. 1a

显的轴部重磁异常条带,宽约 60 ~ 120km,呈对称分布(图 3)。往南重磁异常条带收窄,至 15°N 时完全消失,这可以解释前人将 15°N 视为红海裂谷的南界。北段和中北段重磁异常分布比较杂乱,偶见有 NE-SW 向横穿裂谷的条带,条带在离岸 50 ~ 70km 处消失,可能指示海底扩张方向和起始时间。

按最新的磁异常数据,可以推测整个红海可能存在沿轴的磁异常区(Issachar *et al.*, 2022),这与 Augustin *et al.* (2021)有关垂直重力梯度数据的研究结果相符合。Augustin *et al.* (2021)通过分析地震和垂向重力梯度数据,结合高精度海底地形,认为红海整个裂谷都存在海底扩张形成的洋壳,且洋壳宽度 103 ~ 174km,北部较窄,南部较宽(图 4)。不过,在红海海域范围,洋壳宽度在 17°N 附近达到最大,往南逐渐收窄,这似乎与 Molnar *et al.* (2020)的模拟结果相背,也与一般洋脊的渐进式传播方式矛盾。这主要是由于南段扩张中心发生跃迁引起的,目前红海裂谷南段的扩张中心已从曼德海峡转移至 Manda Hararo 裂谷带,形成阿法尔凹陷(McClusky *et al.*, 2010; Illsley-Kemp *et al.*, 2018)。南段的实际扩张区包括曼德海峡和阿法尔凹陷,扩张区两侧的共轭陆缘距离达 560km,红海北段的拉张量约 200km。因此,红海的扩张整体呈现北部窄、南部宽的喇叭口模式,与我国南海西南次海盆的喇叭口式扩张相似(丁巍伟,2021)。

3 玄武岩地球化学特征及地幔不均一性

海底玄武岩的特征可以反映洋壳的岩浆过程和源区组成。前人对红海裂谷的玄武岩开展了较系统的地球化学研究,讨论了裂谷岩浆演化、南段火山岛成因、地幔柱与洋脊相互作用和地幔不均一性等问题(Gass *et al.*, 1973; Altherr *et al.*, 1988, 1990; Eissen *et al.*, 1989; Rogers, 1993; Volker *et al.*, 1993; Haase *et al.*, 2000)。不过,已有的研究主要基于局部的岩石样品,对全段玄武岩地球化学数据的总结分析有限。

综合红海全段的玄武岩数据(表 1),可以发现红海中北段和中南段为典型的 N-MORB,低的 K/Ti 和 La/Sm 比值。南段和北段显示 E-MORB 特征,17°N 以南尤其明显,富集 K_2O、P_2O_5、TiO_2,具有高的 K/Ti、La/Sm 比值和 Na_8 值(图 5)。并且,南段具有升高的 $^{87}Sr/^{86}Sr$ 比值和 $^{206}Pb/^{204}Pb$ 比值,最高的 Pb 同位素比值位于 17°N 附近的 Ramad 海山,

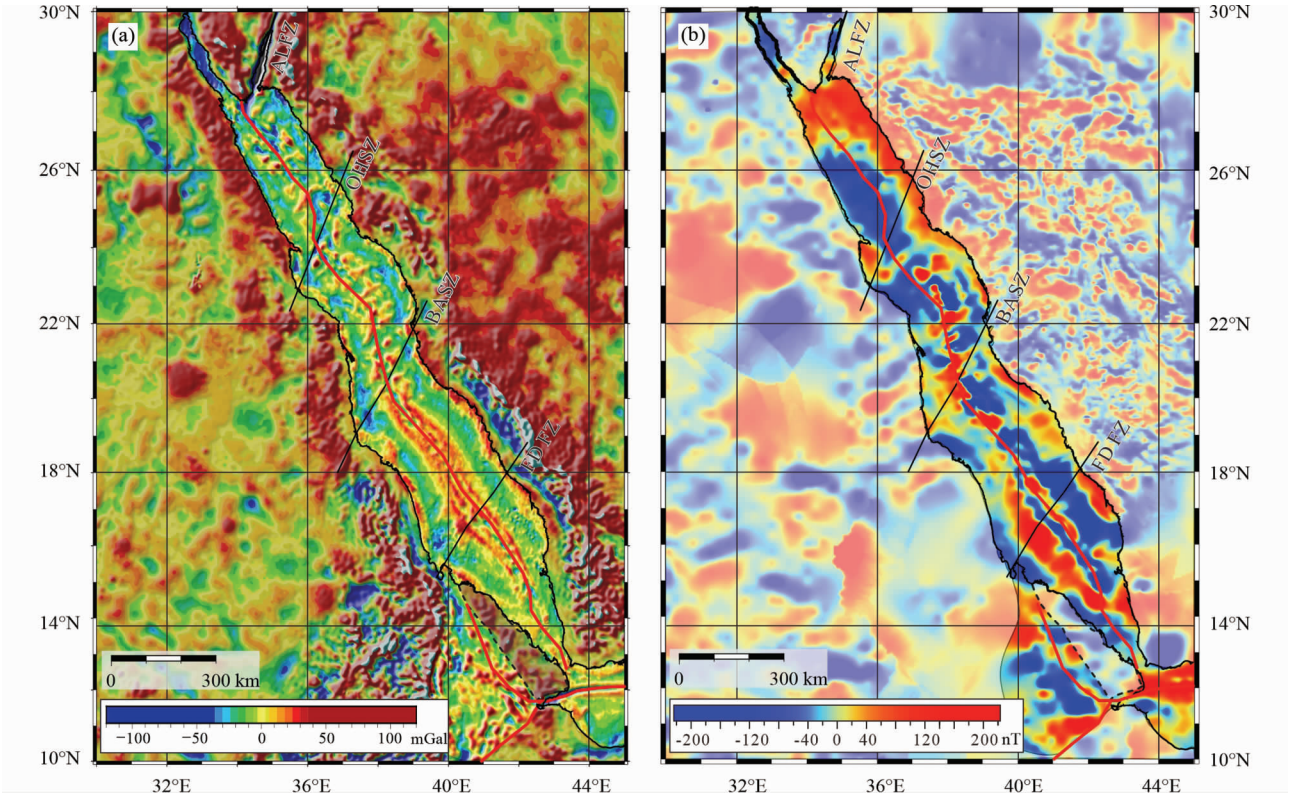

图 3 红海及周边重磁异常图

(a)红海自由空间重力异常图,重力异常数据来自 TOPEX V30(Sandwell *et al.*,2014),红线为扩张中心,黑色线段为分段界线,红海南部虚线区域为达纳基尔(Danakil)地块,地块西南部存在大陆张裂;(b) 红海磁力异常图,磁异常数据来自 EMAG2 v3 全球地磁异常数据集(Meyer *et al.*,2017)

Fig. 3 The free-air gravity anomalies and magnetic anomalies for the Red Sea and adjacent areas

(a) gravity anomalies of the Red Sea. Gravity data are from TOPEX version 30 (Sandwell *et al.*, 2014). The red line indicates the spreading center, and the black line the segment boundary. The block outlined by thin dashed line to the southwest of the Red Sea is the Danakil block, southwest of which is undergoing continental rifting and crust thinning. (b) magnetic anomaly Map of the Red Sea. The magnetic data are from the global geomagnetic anomaly dataset EMAG2 v3 (Meyer *et al.*, 2017)

$^{206}Pb/^{204}Pb$、$^{207}Pb/^{204}Pb$ 和 $^{208}b/^{204}Pb$ 比值分别可达 19.6、15.67 和 39.5(Volker *et al.*,1993,1997)。红海南段玄武岩的地球化学特征显示与阿法尔热点的相似性,指示了阿法尔地幔柱的影响。红海中北段与中南段虽然具有不同的重磁异常特征,但却具有比较均一的化学组成,相对南北两段具有较低的 $^{87}Sr/^{86}Sr$ 比值和 Pb 同位素比值,较高的 $^{143}Nd/^{144}Nd$ 比值(图 5),显示相对亏损的地幔源区,这与中北段和中南段海渊密集分布的特征相符,也表明洋脊发育相对成熟。

红海与东非大裂谷、亚丁湾相交于阿法尔三联点,三者代表了威尔逊旋回的不同阶段(李江海等,2015;李三忠等,2018;吴福元等,2020)。东非大裂谷处于胚胎期,大陆张裂阶段。亚丁湾处于幼年期,已经开始海底扩张。亚丁湾的大陆张裂可能始于 30Ma(Bosworth,2015),与红海相当,同属于阿拉伯半岛与非洲分离并发生逆时针旋转的结果。亚丁湾以阿卢拉-法塔克断裂带为界分为东西两段,东部希贝海脊的最早海底扩张时间为 17.6Ma,西部亚丁海脊的扩张时间~16Ma (Leroy *et al.*,2004; 余星等,2019),均略早于红海。亚丁湾自东向西传播的海底扩张与红海自南向北的渐次扩张相吻合。相似的扩张背景使红海和亚丁湾具有相似的地幔源区特征,均具有相对东非大裂谷更低的 $^{87}Sr/^{86}Sr$ 比值,更高的 $^{143}Nd/^{144}Nd$ 比值(表 1、图 6),表明源区以相对亏损的软流圈地幔为主体,与 MORB 地幔相当。而东非大裂谷的火山作用均发生于大陆环境,具有类似 OIB 的微量元素特征,$(La/Sm)_N$ 为 1~4.6,富集放射性成因同位素(Rogers *et al.*,2000)。红海南段、亚丁湾西部以及东非大裂谷北部均表现出类似阿法尔热点的富集特征,表明阿法尔地幔柱广泛影响了三联点及周边区域,影响半径达 800~1000km(图 6)。

4 红海裂谷演化历史

由于红海洋壳分布范围的不确定性,整个红海裂谷的发育历史仍存在争议。众多学者认为红海初始扩张在~5Ma,且发生在中南部(Courtillot,1982; Cochran,1983; Bosworth *et al.*,2005; Almalki *et al.*,2016);近年来,Augustin *et al.*(2021)

表 1 红海及周边扩张中心玄武岩的主要地球化学参数

Table 1 Main geochemical proxies of the axial basalts from the Red Sea and adjacent areas

洋脊段	红海北段	红海中北段和中南段	红海南段	亚丁湾	东非大裂谷
	24°N 以北	24° ~ 17°N	17°N 以南		
$^{87}Sr/^{86}Sr$	0.703046 ~ 0.70357(12)	0.70240 ~ 0.70305(18)	0.703125 ~ 0.70380(14)	0.70278 ~ 0.70344(33)	0.70303 ~ 0.70668(541)
$^{143}Nd/^{144}Nd$	0.51302 ~ 0.51311(11)	0.51299 ~ 0.51319(17)	0.51295 ~ 0.51308(13)	0.51287 ~ 0.51317(31)	0.51251 ~ 0.51316(430)
$^{206}Pb/^{204}Pb$	18.266 ~ 18.859(4)	18.040 ~ 19.163(19)	18.757 ~ 19.608(14)	18.196 ~ 19.405(31)	16.948 ~ 20.435(321)
$^{207}Pb/^{204}Pb$	15.561 ~ 15.600	15.480 ~ 15.622	15.547 ~ 15.646	15.430 ~ 15.616	15.460 ~ 15.777
$^{208}Pb/^{204}Pb$	37.978 ~ 38.770	37.808 ~ 38.895	38.517 ~ 39.510	37.984 ~ 39.420	37.550 ~ 42.983
Δ7/4	+2.6 ~ +12.4(4)	+0.6 ~ +12.3(19)	−0.89 ~ +8.9(14)	−5.9 ~ +3.4(31)	0 ~ +15(321)
Δ8/4	+25.4 ~ +34.2	+1.1 ~ +41.3	+15.8 ~ +29.6	+10.1 ~ +46.2	−30 ~ +130
Na_8	1.6 ~ 3.3(42)	1.3 ~ 4.6(189)	1.5 ~ 5.3(68)	1.4 ~ 4.0(51)	−0.1 ~ 5.4(1237)
$(La/Sm)_N$	0.6 ~ 1.33(25)	0.18 ~ 1.09(41)	2.2 ~ 3.3(17)	0.4 ~ 4.0(91)	1 ~ 4.6(399)

注:Δ7/4 和 Δ8/4 指示 Pb 同位素相对 NHRL 的偏离度(Hart,1984),Na_8 计算依据 Klein and Langmuir(1987). 括号内数字为统计的数据量. 数据来源于 PetDB

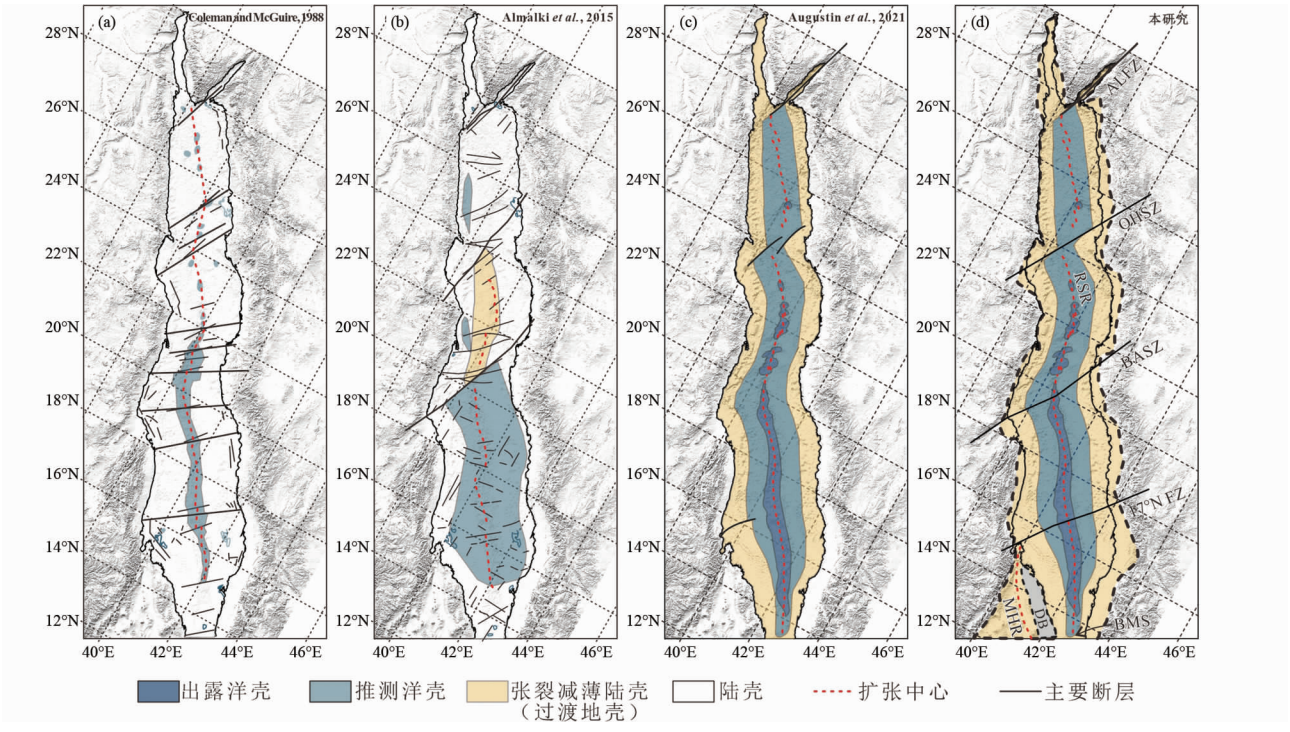

图 4 红海洋壳分布模式对比图

(a)北部存在零星洋壳;(b)北部为陆壳,中部存在过渡地壳;(c)全段存在洋壳;(d)全段存在洋壳及更宽的大陆张裂区. 沿岸的细黑色曲线为海岸线,黑色粗虚线为推测的共轭陆缘(近似 1000m 等高线). DB-达纳基尔(Danakil)地块; BMS-曼德海峡; OHSZ-Onib-Hamisana 缝合带(Zabargad 断裂带); BASZ-Baraka 缝合带; 17°N FZ-17°N 断裂带; ALFZ-亚喀巴-黎凡特(Aqaba-Levant)断层; MHR-Manda Hararo 裂谷带; RSR-红海裂谷

Fig. 4 Comparison of the oceanic crust distribution models of the Red Sea

(a) scattered oceanic crust occurred in the north; (b) continental crust in the north with transitional crust in the middle section; (c) oceanic crust throughout the rift; (d) oceanic crust exists throughout the rift with broader area of continental rifting and crust thinning. The thin black curves are the coastlines, while the bold black dashed lines represent the conjugated margins, approximate to the 1000m contour. DB-Danakil Block; BMS-Bab al-Mandab Strait; OHSZ-Onib-Hamisana Suture Zone (Zabargad Fracture Zone); BASZ-Baraka Suture Zone; 17°N FZ-17°N Fracture Zone; ALFZ-Aqaba-Levant Fracture Zone; MHR-Manda Hararo Rift Zone; RSR-Red Sea Rift

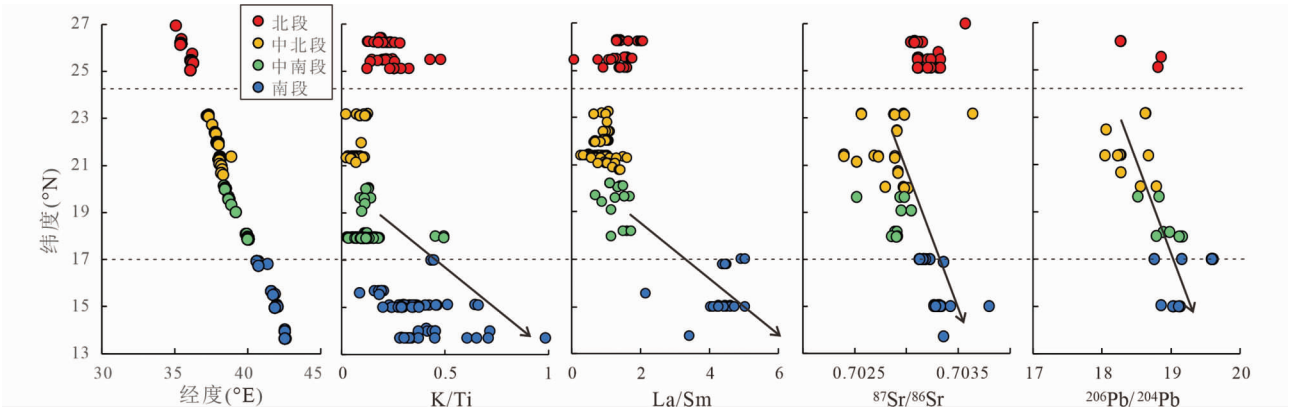

图 5　红海玄武岩沿轴的地球化学特征(数据来源于 PetDB)

Fig. 5　The geochemical variations of the Red Sea basalts along the rift axis (the geochemical data from PetDB)

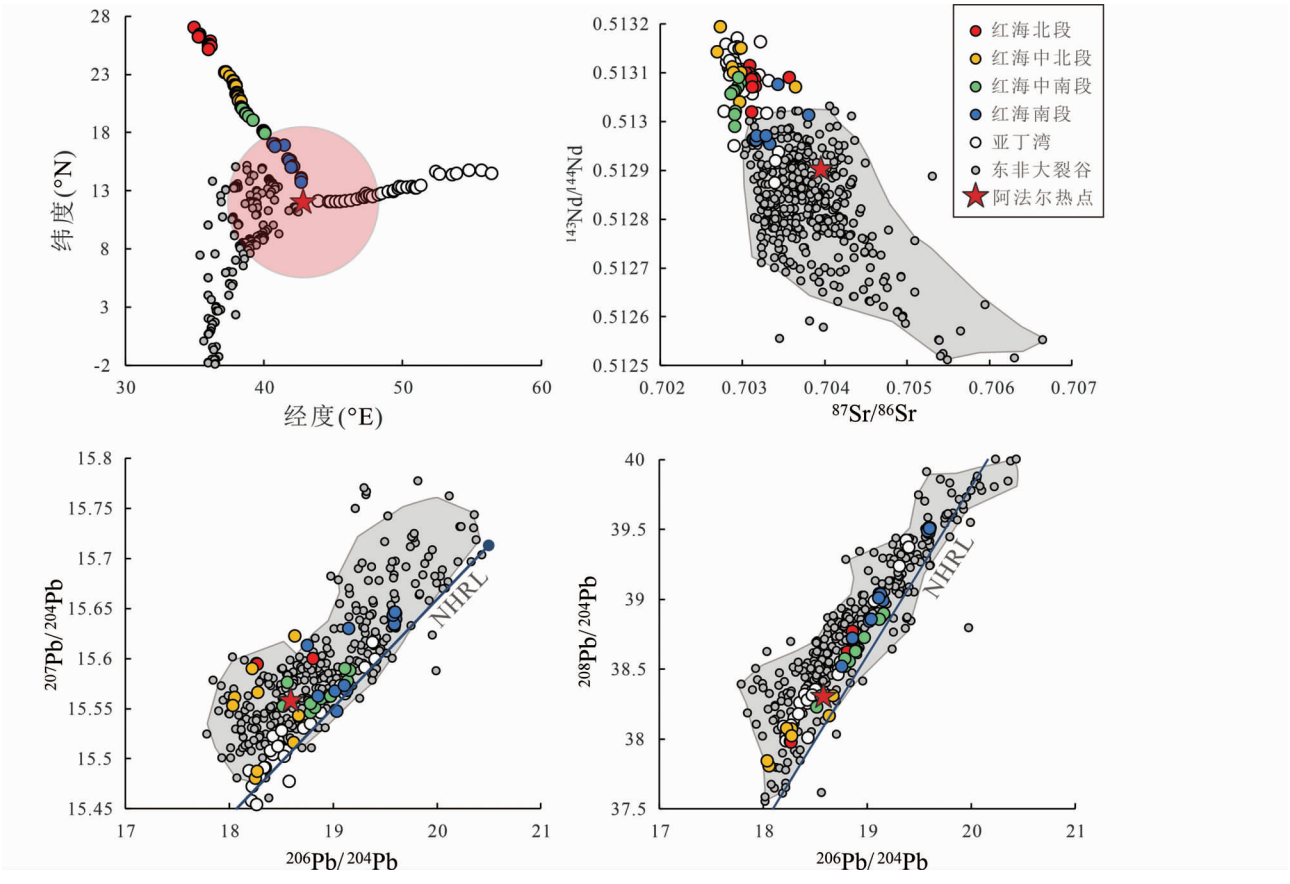

图 6　红海与周边扩张中心玄武岩同位素关系图

红色阴影区为推测阿法尔热点影响区，灰色阴影区域为东非大裂谷玄武岩的同位素分布范围. 数据来源于 PetDB，阿法尔热点同位素数据据 Baker *et al*. (1996)

Fig. 6　The isotopic compositions of the basalts from Red Sea and adjacent areas

The shaded red area indicates the prospective affected region by Afar hotspot. The shaded grey area indicates the isotope distribution range of the basalts from East African Rift. The geochemical data for the basalts from PetDB, while the isotopic data for Afar hotspot from Baker *et al*. (1996)

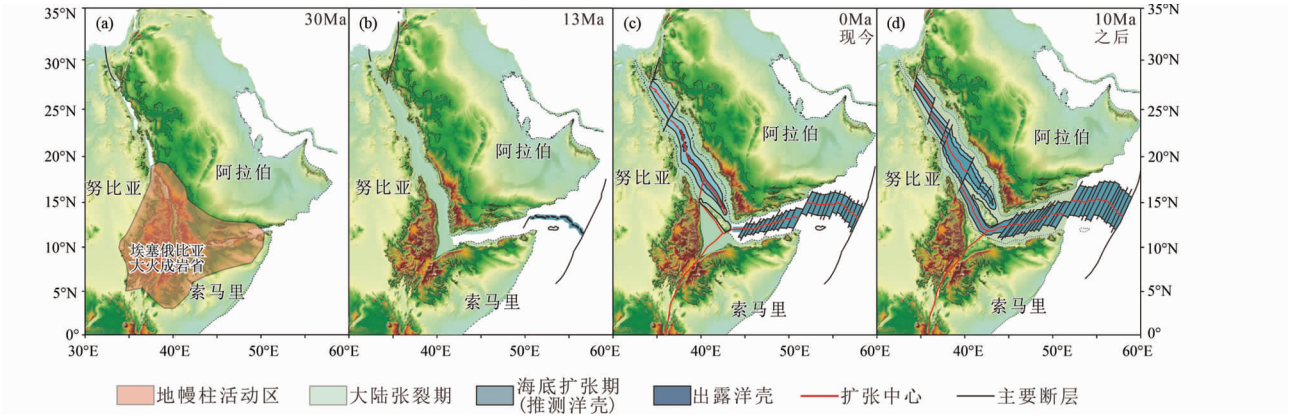

图 7 红海裂谷演化过程示意图

以非洲大陆为参考点,未考虑努比亚板块和索马里板块间的相对扩张. 演化模式综合了 Bosworth *et al.* (2005), Almalki *et al.* (2015), Schettino *et al.* (2019), Molnar *et al.* (2020), Augustin *et al.* (2021) 和 Boone *et al.* (2021)等的研究结果

Fig. 7 The sketch maps of evolution of the Red Sea Rift

The fixed reference for the model is the African continent. The simplified model has not taken the relative motion between the Nubian and Somali plates into account. This evolutionary model has integrated the results of Bosworth *et al.* (2005), Almalki *et al.* (2015), Schettino *et al.* (2019), Molnar *et al.* (2020), Augustin *et al.* (2021) and Boone *et al.* (2021), etc.

则认为红海初始扩张始于 ~13Ma,且全段都已开始海底扩张。综合前人的研究成果,基于区域的地质构造特征和洋壳分布模式,本文认为红海裂谷的发育经历了裂谷前火山作用、大陆张裂和洋底扩张三个主要阶段(图 7)。

第一阶段为裂谷前火山作用,发生在 31 ~29Ma。31Ma 前后,阿法尔地幔柱开始在埃塞俄比亚、苏丹东北部和也门西南部等地上涌,形成面积达 $6\times105km^2$ 的埃塞俄比亚大火成岩省(图 7a),或称非洲-阿拉伯大火成岩省(Cochran, 2005; Prave *et al.*, 2016; Varet, 2018; Thines *et al.*, 2021)。这一时期刚好对应亚丁湾的起始扩张时间(Ghebreab, 1998)。

第二阶段为大陆张裂期,发生在 29 ~13Ma。在这一时期,以阿法尔三联点为中心的三支裂谷(东非大裂谷、红海、亚丁湾)均发生了张裂作用,但具体的时间序列仍不明确。红海的具体起始张裂时间也存在争议(Zanettin *et al.*, 1978; Omar and Steckler, 1995; Kusky *et al.*, 2010),不过均介于 29 ~13Ma 期间。24 ~23Ma 期间,整个红海周边地区出现了以玄武质岩墙、层状辉长岩和花岗岩体为主的新火山作用(Bosworth, 2015),也支持大陆张裂作用。大陆张裂的距离可达 200km 左右(图 7b)。大约在 14 ~12Ma,左行走滑的亚喀巴-黎凡特(Aqaba-Levant)断层开始活动,阿拉伯半岛顺亚喀巴-黎凡特断层的走滑与非洲分离,为红海的海底扩张提供了便利(Bosworth, 2015)。

第三阶段为洋底扩张期,发生在 ~13Ma 以来。亚喀巴-黎凡特断层的活动,相对加速了阿拉伯板块的北东向漂移,这与 Augustin *et al.* (2021)提出的 ~13Ma 时红海全域进入洋底扩张相符。红海南部与北部的起始洋底扩张时间相同,扩张速度南部较北部快,全扩张速度分别为 13mm/yr 和 8mm/yr,南部洋壳宽约 170km,北部宽 100km(Augustin *et al.*, 2021)。红海北部的扩张方向为 N15°E,南部近 N45°E(图 7c),这与阿拉伯板块的逆时针旋转有关,同时解释了亚喀巴湾向南开口的特征。

红海的扩张总体呈向南开口的喇叭型,而非红海岸线所围限的梭子型,这与 Molnar *et al.* (2020)的模拟结果相符。红海南部 15°N 以南未见有明显的洋壳痕迹,这可能扩张中心跃迁、埃塞俄比亚大火成岩省以及阿尔法地幔柱的火山活动有关。大火成岩省区域陆壳较厚,可能需要更长久的陆壳减薄过程;另一方面,持续的地幔柱火山活动会掩盖海底扩张作用,地球化学证据支持地幔柱对红海南段的影响。但南段的大陆张裂作用非常明显,共轭陆缘(也门西南角与阿尔法凹陷西南角)扩张了约 560km。红海南端的海底扩张中心在 ~7Ma 发生了跃迁,在达纳基尔地块西部发育新的扩张边界——Manda Hararo 裂谷带(Audin *et al.*, 2004),密集分布的地震活动可以证实。红海南部的扩张边界穿过阿法尔凹陷分别与东非大裂谷、亚丁湾相连,形成阿法尔三联点。推测未来红海的扩张将通过 Manda Hararo 裂谷带与亚丁湾相接,达纳基尔地块可能会成为阿拉伯板块的一部分(图 7d)。

5 结论与展望

通过系统分析红海及周边地区的地形地貌、重磁异常、玄武岩地球化学组成等资料,对红海地区的地质构造特征有了更全面的认识,对红海裂谷的分段、洋壳分布、扩张历史以及地幔源区不均一性等问题进行了多角度的交叉探讨,取得了以下认识:

(1)红海整体可以分为北、中北、中南、南等四段,分别以 24°N、20°N 和 17°N 为界。南北两段水深较浅,中间较深,玄

武岩球化学特征也显示沿轴的差异。红海最显著的重磁异常特征表现为中南段具有明显的轴部重磁异常条带，而其他段则比较杂乱。

(2)红海全段存在洋壳，中南段尤其明显，而且洋壳宽度大于预期。红海南段洋壳宽度较小，是由于洋脊跃迁和地幔柱活动的共同影响，南段共轭陆缘的张裂距离达560km。

(3)红海不同裂谷段具有地幔源区不均一性，中北段和中南段相对亏损，南北两段相对富集。红海南段与亚丁湾西部以及东非大裂谷的北部均受到阿法尔地幔柱的影响，表现出明显的E-MORB特征，富集放射性成因同位素。

(4)红海的扩张经历了裂谷前火山作用、大陆张裂和洋底扩张三个主要阶段。第一阶段31～29Ma，阿法尔地幔柱活动形成埃塞俄比亚大火成岩省；第二阶段29～13Ma，以阿法尔三联点为中心的三支裂谷均发生了张裂作用；第三阶段13Ma以来，伴随着亚喀巴-黎凡特断层的活动，红海全段开始海底扩张。红海扩张并非是两端窄、中间宽的梭子型，而是由北向南开口的喇叭型。

由于红海内厚层沉积物的覆盖、基底岩石取样的不足和地球物理资料的多解性，有关红海裂谷的洋壳分布范围、扩张演化历史等仍需进一步研究证实。未来，增加新的深部大洋钻探，开展高精度的近底地球物理探测，将为红海裂谷的深入研究提供新的动力。

致谢 感谢自然资源部第二海洋研究所王叶剑和吴招才研究员在红海裂谷演化及地球物理资料解译方面的讨论与指导；感谢两位匿名评审人对本文提出的宝贵修改意见。

References

Allan TD. 1970. A discussion on the structure and evolution of the Red Sea and the nature of the Red Sea, gulf of Aden and Ethiopia rift junction: Magnetic and gravity fields over the Red Sea. Philosophical Transactions of the Royal Society of London. Series A, Mathematical and Physical Sciences, 267(1181): 153 – 180

Almalki KA, Betts PG and Ailleres L. 2015. The Red Sea: 50 years of geological and geophysical research. Earth-Science Reviews, 147: 109 – 140

Almalki KA, Betts PG and Ailleres L. 2016. Incipient seafloor spreading segments: Insights from the Red Sea. Geophysical Research Letters, 43(6): 2709 – 2715

Altherr R, Henjes-Kunst F, Puchelt H and Baumann A. 1988. Volcanic activity in the Red Sea axial trough: Evidence for a large mantle diapir? Tectonophysics, 150(1 – 2): 121 – 133

Altherr R, Henjes-Kunst F and Baumann A. 1990. Asthenosphere versus lithosphere as possible sources for basaltic magmas erupted during formation of the Red Sea: Constraints from Sr, Pb and Nd isotopes. Earth and Planetary Science Letters, 96(3 – 4): 269 – 286

Audin L, Quidelleur X, Coulié E, Courtillot V, Gilder S, Manighetti I, Gillot PY, Tapponnier P and Kidane T. 2004. Palaeomagnetism and K-Ar and $^{40}Ar/^{39}Ar$ ages in the Ali Sabieh area (Republic of Djibouti and Ethiopia): Constraints on the mechanism of Aden ridge propagation into southeastern Afar during the last 10Myr. Geophysical Journal International, 158(1): 327 – 345

Augustin N, Devey CW, van der Zwan FM, Feldens P, Tominaga M, Bantan RA and Kwasnitschka T. 2014. The rifting to spreading transition in the Red Sea. Earth and Planetary Science Letters, 395: 217 – 230

Augustin N, Devey CW and Van der Zwan FM. 2019. A modern view on the Red Sea rift: Tectonics, volcanism and salt blankets. In: Rasul NMA and Stewart ICF (eds.). Geological Setting, Palaeoenvironment and Archaeology of the Red Sea. Switzerland: Springer, 37 – 52

Augustin N, van der Zwan FM, Devey CW and Brandsdóttir B. 2021. 13 million years of seafloor spreading throughout the Red Sea Basin. Nature Communications, 12: 2427

Bäcker H and Schoell M. 1972. New deeps with brines and metalliferous sediments in the Red Sea. Nature Physical Science, 240(103): 153 – 158

Baker JA, Thirlwall MF and Menzies MA. 1996. Sr-Nd-Pb isotopic and trace element evidence for crustal contamination of plume-derived flood basalts: Oligocene flood volcanism in western Yemen. Geochimica et Cosmochimica Acta, 60(14), 2559 – 2581

Belogorskaya EV. 1970. Qualitative and quantitative distribution of phytoplankton in the Red Sea and Gulf of Aden in October-November 1963. Marine Biology, 21: 133 – 152

Bonatti E, Colantoni P, Della Vedova B and Taviani M. 1984. Geology of the Red Sea transitional region (22° N ~ 25° N). Oceanologica Acta, 7(4): 385 – 398

Boone SC, Balestrieri ML and Kohn B. 2021. Thermo-tectonic imaging of the Gulf of Aden-Red Sea rift systems and Afro-Arabian hinterland. Earth-Science Reviews, 222: 103824

Bosworth W, Huchon P and McClay K. 2005. The Red Sea and Gulf of Aden basins. Journal of African Earth Sciences, 43(1 – 3): 334 – 378

Bosworth W. 2015. Geological evolution of the Red Sea: Historical background, review, and synthesis. In: Rasul NMA and Stewart ICF (eds.). The Red Sea. Berlin, Heidelberg: Springer, 45 – 78

Brueckmann W, Kraetschell A and Augustin N. 2017. Data mining the Red Sea Atlantis II deep. In: Offshore Technology Conference. Houston, Texas, USA

Cochran JR. 1983. A model for development of Red Sea. AAPG Bulletin, 67(1): 41 – 69

Cochran JR, Martinez F, Steckler MS and Hobart MA. 1986. Conrad deep: A new northern Red Sea deep: Origin and implications for continental rifting. Earth and Planetary Science Letters, 78(1): 18 – 32

Cochran JR. 2005. Northern Red Sea: Nucleation of an oceanic spreading center within a continental rift. Geochemistry, Geophysics, Geosystems, 6(3): Q03006

Coleman RG and McGuire AV. 1988. Magma systems related to the Red Sea opening. Tectonophysics, 150(1 – 2): 77 – 100

Courtillot V. 1982. Propagating rifts and continental breakup. Tectonics, 1(3): 239 – 250

Ding WW. 2021. Continental margin dynamics of South China Sea: from continental break-up to seafloor spreading. Earth Science, 46(3): 790 – 800 (in Chinese with English abstract)

Eissen JP, Juteau T, Joron JL, Dupre B, Humler E and Al'mukhamedov A. 1989. Petrology and geochemistry of basalts from the Red Sea axial rift at 18° North. Journal of Petrology, 30(4): 791 – 839

Gass IG, Mallick DIJ and Cox KG. 1973. Volcanic islands of the Red Sea. Journal of the Geological Society, 129(3): 275 – 309

Ghebreab W. 1998. Tectonics of the Red Sea region reassessed. Earth-Science Reviews, 45(1 – 2): 1 – 44

Girdler RW. 1958. The relationship of the Red Sea to the East African Rift system. Quarterly Journal of the Geological Society, 114(1 – 4): 79 – 105

Haase KM, Mühe R and Stoffers P. 2000. Magmatism during extension of the lithosphere: Geochemical constraints from lavas of the Shaban Deep, northern Red Sea. Chemical Geology, 166(3 – 4): 225 – 239

Hall SA. 1979. A Total Intensity Magnetic Anomaly Map of the Red Sea and Its Interpretation. Saudi Arabia: U. S. Geological Survey, 260 – 275

Hart SA. 1984. Large-scale isotope anomaly in the Southern Hemisphere

mantle. Nature, 309: 753 – 757
Head SM. 1987. Red Sea fisheries. In: Edwards AJ and Head SM (eds.) Red Sea: Key Environments Series. Oxford: Pergamon Press, 363 – 382
Huang YQ and Hou DJ. 2006. Genetic analysis and evolution of the Red Sea Rift Basin. In: Proceedings of the Earth Sciences Sub-Forum, at National Doctoral Academic Forum 2006. Beijing, 155 – 160 (in Chinese)
Illsley-Kemp F, Keir D, Bull JM, Gernon TM, Ebinger C, Ayele A, Hammond JOS, Kendall JM, Goitom B and Belachew M. 2018. Seismicity during continental breakup in the Red Sea rift of Northern Afar. Journal of Geophysical Research: Solid Earth, 123(3): 2345 – 2362
Issachar R, Ebbing J and Dilixiati Y. 2022. New magnetic anomaly map for the Red Sea reveals transtensional structures associated with rotational rifting. Scientific Reports, 12(1): 5757
Izzeldin AY. 1987. Seismic, gravity and magnetic surveys in the central part of the Red Sea: Their interpretation and implications for the structure and evolution of the Red Sea. Tectonophysics, 143(4): 269 – 306
Klein EM and Langmuir CH. 1987. Global correlations of ocean ridge basalt chemistry with axial depth and crustal thickness. Journal of Geophysical Research: Solid Earth, 92(B8): 8089 – 8115
Kusky TM, Toraman E, Raharimahefa T and Rasoazanamparany C. 2010. Active tectonics of the Alaotra-Ankay Graben System, Madagascar: Possible extension of Somalian-African diffusive plate boundary? Gondwana Research, 18(2 – 3): 274 – 294
Le Pichon X and Francheteau J. 1978. A plate-tectonic analysis of the Red Sea-Gulf of Aden area. Tectonophysics, 46(3 – 4): 369 – 406
Leroy S, Gente P, Fournier M, d'Acremont E, Patriat P, Beslier MO, Bellahsen N, Maia M, Blais A, Perrot J, Al-Kathiri A, Merkouriev S, Fleury JM, Ruellan PY, Lepvrier C and Huchon P. 2004. From rifting to spreading in the eastern Gulf of Aden: A geophysical survey of a young oceanic basin from margin to margin. Terra Nova, 16(4): 185 – 192
Li JB. 2017. Geology of the Modern Submarine Hydrothermal Sulfide Mineralization. Beijing: Science Press, 1 – 313 (in Chinese)
Li JH, Zhang HT and Li HL. 2015. The tectonic setting and evolution of Indian Ocean: Research progress of tectonic map of Indian Ocean. Haiyang Xuebao, 37(7): 1 – 14 (in Chinese with English abstract)
Li SZ, Zhao SJ, Suo YH, Liu B and Li XY. 2018. Regional Submarine Tectonics: Volume One. Beijing: Science Press, 1 – 296 (in Chinese)
Ligi M, Bonatti E, Bortoluzzi G, Cipriani A, Cocchi L, Tontini FC, Carminati E, Ottolini L and Schettino A. 2012. Birth of an ocean in the Red Sea: Initial pangs. Geochemistry, Geophysics, Geosystems, 13(8): Q08009
Makris J, Mohr P and Rihm R. 1991. Red Sea: Birth and early history of a new oceanic basin. Tectonophysics, 198(2 – 4): 129 – 468
McClusky S, Reilinger R, Ogubazghi G, Amleson A, Healeb B, Vernant P, Sholan J, Fisseha S, Asfaw L, Bendick R and Kogan L. 2010. Kinematics of the southern Red Sea-Afar triple junction and implications for plate dynamics. Geophysical Research Letters, 37(5): L05301
McKenzie DP, Davies D and Molnar P. 1970. Plate tectonics of the Red Sea and East Africa. Nature, 226(5242): 243 – 248
Meyer B, Saltus R and Chulliat A. 2017. EMAG2v3: Earth Magnetic Anomaly Grid (2-arc-minute resolution). Version 3. NOAA National Centers for Environmental Information
Molnar N, Cruden A and Betts P. 2020. The role of inherited crustal and lithospheric architecture during the evolution of the Red Sea: Insights from three dimensional analogue experiments. Earth and Planetary Science Letters, 544: 116377
Omar GI and Steckler MS. 1995. Fission track evidence on the initial rifting of the Red Sea: Two pulses, no propagation. Science, 270(5240): 1341 – 1344
Phillips JD, Woodside J and Bowin CO. 1969. Magnetic and gravity anomalies in the central Red Sea. In: Degens ET and Ross DA (eds.). Hot Brines and Recent Heavy Metal Deposits in the Red Sea. Berlin, Heidelberg: Springer, 98 – 113
Prave AR, Bates CR, Donaldson CH, Toland H, Condon DJ, Mark D and Raub TD. 2016. Geology and geochronology of the Tana Basin, Ethiopia: LIP volcanism, super eruptions and Eocene-Oligocene environmental change. Earth and Planetary Science Letters, 443: 1 – 8
Rasul NMA, Stewart ICF and Nawab ZA. 2015. Introduction to the Red Sea: Its origin, structure, and environment. In: Rasul NMA and Stewart ICF (eds.). The Red Sea. Berlin, Heidelberg: Springer, 1 – 28
Rogers N, Macdonald R, Fitton JB, George R, Smith M and Barreiro B. 2000. Two mantle plumes beneath the East African rift system: Sr, Nd and Pb isotope evidence from Kenya Rift basalts. Earth and Planetary Science Letters, 176(3 – 4): 387 – 400
Rogers NW. 1993. The isotope and trace element geochemistry of basalts from the volcanic islands of the southern Red Sea. In: Prichard HM, Alabaster T, Haris NB and Neary CR (eds.). Magmatic Processes and Plate Tectonics. Geological Society, London, Special Publications, 76(1): 455 – 467
Saada SA, Mickus K, Eldosouky AM and Ibrahim A. 2021. Insights on the tectonic styles of the Red Sea rift using gravity and magnetic data. Marine and Petroleum Geology, 133: 105253
Sandwell DT, Müller RD, Smith WHF, Garcia E and Francis R. 2014. New global marine gravity model from CryoSat-2 and Jason-1 reveals buried tectonic structure. Science, 346(6205): 65 – 67
Schettino A, Macchiavelli C, Pierantoni PP, Zanoni D and Rasul N. 2016. Recent kinematics of the tectonic plates surrounding the Red Sea and Gulf of Aden. Geophysical Journal International, 207(1): 457 – 480
Schettino A, Macchiavelli C and Rasul NMA. 2019. Plate motions around the Red Sea since the Early Oligocene. In: Rasul NMA and Stewart ICF (eds.). Geological Setting, Palaeoenvironment and Archaeology of the Red Sea. Switzerland: Springer, 203 – 220
Scholten JC, Staffers P, Garbe-Schdnberg D and Moammar M. 2000. Hydrothermal mineralization in the Red Sea. In: Cronan DS (eds.). Handbook of Marine Mineral Deposits. London: Routledge, 369 – 395
Thines JE, Ukstins IA, Wall C and Schmitz M. 2021. Volumetric extrusive rates of silicic super-eruptions from the Afro-Arabian large igneous province. Nature Communications, 12(1): 6299
Tozer B, Sandwell DT, Smith WHF, Olson C, Beale JR and Wessel P. 2019. Global bathymetry and topography at 15 arc sec: SRTM15 +. Earth and Space Science, 6(10): 1847 – 1864
Varet J. 2018. Geophysical frame: Mantle plume(s), triple points, rifting processes. In: Varet J (ed.). Geology of Afar (East Africa). Cham.: Springer, 39 – 54
Volker F, McCulloch MT and Altherr R. 1993. Submarine basalts from the Red Sea: New Pb, Sr, and Nd isotopic data. Geophysical Research Letters, 20(10): 927 – 930
Volker F, Altherr R, Jochum KP and McCulloch MT. 1997. Quaternary volcanic activity of the southern Red Sea: New data and assessment of models on magma sources and Afar plume-lithosphere interaction. Tectonophysics, 278(1 – 4): 15 – 29
Wu FY, Wan B, Zhao L, Xiao WJ and Zhu RX. 2020. Tethyan geodynamics. Acta Petrologica Sinica, 36(6): 1627 – 1674 (in Chinese with English abstract)
Yu X, Han XQ, Qiu ZY, Wang YJ and Tang LM. 2019. Definition of Northwest Indian ridge and its geologic and tectonic signatures. Earth Science, 44(2): 626 – 639 (in Chinese with English abstract)
Zanettin B, Justin-Visentin E and Piccirillo EM. 1978. Volcanic Succession, Tectonics and Magmatology in Central Ethiopia. Milano: Tipografia degli Operai, 1 – 15
Zeng ZG. 2011. Submarine Hydrothermal Geology. Beijing: Science Press, 1 – 567 (in Chinese)

附中文参考文献

丁巍伟, 2021. 南海大陆边缘动力学:从陆缘破裂到海底扩张. 地球

科学，46(3)：790－800
黄彦庆，侯读杰. 2006. 红海裂谷盆地的成因分析及其演化过程. 见：2006 年全国博士生学术论坛——地球科学分论坛论文集. 北京，155－160
李家彪. 2017. 现代海底热液硫化物成矿地质学. 北京：科学出版社，1－313
李江海，张华添，李洪林. 2015. 印度洋大地构造背景及其构造演化——印度洋底大地构造图研究进展. 海洋学报，37(7)：1－14
李三忠，赵淑娟，索艳慧，刘博，李玺瑶. 2018. 区域海底构造(上). 北京：科学出版社，1－296
吴福元，万博，赵亮，肖文交，朱日祥. 2020. 特提斯地球动力学. 岩石学报，36(6)：1627－1674
余星，韩喜球，邱中炎，王叶剑，唐立梅. 2019. 西北印度洋脊的厘定及其地质构造特征. 地球科学，44(2)：626－639
曾志刚. 2011. 海底热液地质学. 北京：科学出版社，1－567